Angewandte Chemie
Eine Zeitschrift der Gesellschaft Deutscher Chemiker

Supporting Information

69451 Weinheim, Germany

Selective Growth of a Stable Drug Polymorph by Suppressing the Nucleation of Corresponding Metastable Polymorph

Jason R. Cox, Lori A. Ferris and Venkat R. Thalladi*

Department of Chemistry and Biochemistry, Worcester Polytechnic Institute, Worcester, MA 01609

S1. Materials. (2-Carbomethoxy)ethyltrichlorosilane (**3**) was purchased from Oakwood Products Inc. and used as received. (3-Cyanopropyl)trichlorosilane (**4**) and (1*H*,1*H*,2*H*,2*H*-perfluorooctyl)trichlorosilane (**9**) were purchased from Aldrich and used without further purification. (3-Chloropropyl)trichlorosilane (**5**), (4-chloromethyl)phenyltrichlorosilane (**6**), and indomethacin were purchased from Alfa Aesar and used without further purification. 10-Undecenyltrichlorosilane (**7**) was purchased from Gelest Inc. and used as received. *n*-Octadecyltrichlorosilane (**8**) was purchased from TCI America and used as received. Absolute ethanol and HPLC grade toluene were purchased from Pharmco and used as received. Precleaned 25 × 75 × 1 mm and 50 × 75 × 1 mm glass microscope slides were purchased from VWR and ½ dram (1.85 mL), 3 dram (11.09 mL) and 20 mL precleaned glass vials were purchased from Kimble and Wheaton Scientific and used as received. The vials were sold in these different denominations (dram and mL); in the following sections we refer to the vials using the naming given above.

S2. Preparation of Substrates and Plasma Oxidation. Glass microscope slide substrates were prepared by cutting the slides into 1 × 10 × 15 mm strips. These strips and glass vials (to be used as silane substrates) were oxidized for approximately two minutes under an oxygen plasma using a plasma etcher (SPI Plasma Prep II) that was operating at 13.56 MHz under a 200 micron vacuum. Plasma oxidation of glass substrates is a well established process; it creates surfaces exposing silanol groups (Figure S1). After the completion of plasma oxidation, the mild vacuum inside the plasma chamber was maintained (to avoid contamination from outside moisture) until the glass slides and vials were ready for monolayer deposition. All the substrates (slides and vials) were oxidized immediately prior to monolayer deposition.

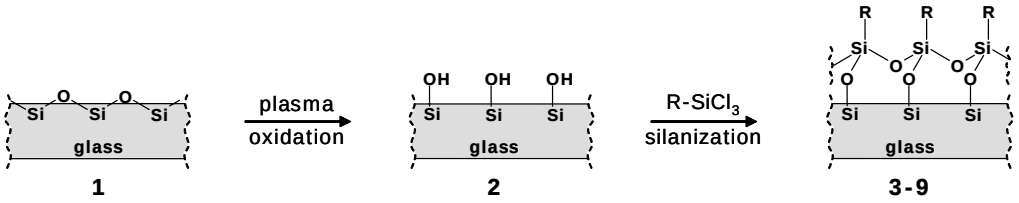

Figure S1. Schematic representation of plasma oxidation of glass substrates and silanization with trichlorosilane derivatives.

S3. Fabrication of Silane Monolayers on Glass Slide Substrates. Trichlorosilane **(**R-$SiCl_3$) solutions (~1 mM) were freshly prepared in toluene and transferred to 20 mL glass vials. Freshly oxidized glass slide strips were removed from the plasma etcher and immersed in the trichlorosilane solutions. The glass vials were completely filled with the silane solutions; they were capped and stored in a cabinet for approximately three hours. The slides were removed from the trichlorosilane solutions, rinsed thoroughly with toluene, and sonicated for 20 minutes in acetone using a Branson 2510 sonicator. After the sonication, the slides were washed with absolute ethanol at least three times and dried under a stream of nitrogen. These slides exposing the silane monolayers at the surface (Figure S1) were used for crystal growth within 30 minutes of the fabrication of the monolayers.

S4. Fabrication of Silane Monolayers on the Inner Surfaces of Glass Vials. Freshly prepared ~1 mM toluene solutions of trichlorosilanes were transferred to oxidized ½ dram glass vials that had just been removed from the plasma chamber. The vials were filled completely with silane solutions, capped, and stored in a cabinet. After three hours, the trichlorosilane solutions were pipetted out of the vials using glass Pasteur pipettes. The vials were rinsed thoroughly with toluene, sonicated for 20 minutes in acetone using a Branson 2510 sonicator, washed at least three times with absolute ethanol and dried under a stream of nitrogen. These vials now contained silane monolayers on their inner surfaces (Figure S1); they were used for crystal growth experiments within 30 minutes of the fabrication of the monolayers.

S5. Contact Angle Measurements. Contact angles were measured at nine different positions for each type of surface (three separate slides) with a manual goniometer (Rame-Hart, Model 100-00). The values reported in Table S1 were averages of these measurements. Deionized water droplets (3 μL) were added to each surface using a calibrated Epindorf pipette and the angles obtained had a maximum error of ± 2.3°. The contact angles show that the surface is modified; they provide a rough measure of hydrophobicity and hydrophilicity of the surfaces.

Table S1. Contact angle data for substrates **1**-**9**.

Substrate	Silane	Contact Angle
1	bare glass	19.3 ± 2.3°
2	plasma treated glass	13.5 ± 2.1°
3	(2-carbomethoxy)ethyltrichlorosilane	42.1 ± 1.8°
4	(3-cyanopropyl)trichlorosilane	56.3 ± 2.2°
5	(3-chloropropyl)trichlorosilane	68.4 ± 1.8°
6	(4-chloromethyl)phenyltrichlorosilane	75.8 ± 1.4°
7	10-undecenyltrichlorosilane	86.7 ± 1.8°
8	*n*-octadecyltrichlorosilane	91.3 ± 1.2°
9	(1*H*,1*H*,2*H*,2*H*-perfluorooctyl)trichlorosilane	104.4 ± 1.1°

S6. Crystal Growth on Glass Slides Bearing Silane Monolayers. In a 100 mL beaker, 25 mM indomethacin solution was made in ethanol and heated at 60 °C for 30 minutes. Ethanol was added in excess at the beginning; the volume of the solution was reduced to required concentration by the evaporation of solvent during heating. The solution was cooled to 20 °C and filtered to 20 mL glass vials containing glass slides bearing silane monolayers. The slides were placed at the bottom of the vial as shown in Figure 1b. Each vial was filled with 5 mL of the solution and covered with a perforated aluminum foil to allow the evaporation of the solvent. All the crystal growth experiments were performed at 20 °C in parallel for at least eight times. The results in all these experiments were qualitatively similar; see Figure 4 and Section S12 below for the quantification of the results. Crystals of α-polymorph appeared on the vial walls within 10-20 hours in all the cases.

S7. Crystal Growth in Glass Vials Functionalized with Silane Monolayers on the Inner Surfaces. Indomethacin solutions (25 mM) were prepared as above and filtered to ½ dram glass vials functionalized with silane monolayers. Each vial was filled with 1.2 mL of the solution and covered with a perforated aluminum foil to allow the slow evaporation of the solvent. All the crystal growth experiments were performed at 20 °C in parallel for at least eight times. The results in all these experiments were qualitatively similar; see Figure 4 and below for the quantification of the results. Crystals of α-polymorph appeared on the walls of vials **1**-**8** within 14-20 hours in all the cases. In **9** vials, crystals of γ-polymorph appeared at the bottom of the vials in 30-56 hours. In these vials crystal growth did not occur on the vial walls. Commercial indomethacin contained predominantly (> 97 %) γ-polymorph. We also carried out crystallizations in **9** vials using indomethacin solutions that were prepared from > 99% α-polymorph. In

three out of three experiments under these conditions, we observed the exclusive crystal growth of γ-polymorph in **9** vials.

S8. Crystal Growth in Functionalized Glass Vials from Acetonitrile Solutions. The procedure is as above except that acetonitrile is used as a solvent instead of ethanol. The concentrations of the solutions were 25 mM. As in the case of ethanol solutions, control vials **1**-**2** and vials functionalized with monolayers **3**-**8** yielded a mixture of α- and γ-polymorphs, whereas the vials functionalized with **9** monolayers produced only the γ-polymorph. We carried out these experiments two times.

S9. Crystal Growth by Slower Evaporation in Functionalized Glass Vials. We did two repeats of these experiments using 25 mM ethanol solutions in functionalized ½ dram vials. We sealed the vials with parafilm and made a pinhole in the parafilm with the tip of a needle. The objective here was to retard the rate of evaporation of ethanol and contrast these results with the experiments above. As above, crystals of α-polymorph grew on the walls of vials **1**-**8** and no crystal growth occurred on the walls of **9** vials. The difference in this case is that α-crystals appeared on the walls of vials **1**-**8** after at least *four days*. In **9** vials, γ-crystals appeared at the bottom after five to six days. These results confirm that the nuclei of α-polymorph survive in solution for at least four days by sticking to the walls of vials **1**-**8**; they do not survive in **9** vials because they cannot attach to the surfaces in these vials. In other words, the growth of γ-polymorph in **9** vials is facilitated by the suppression of hetereogeneous nucleation of α-polymorph. We also carried out crystallizations of indomethacin from 25 mM ethanol solutions in functionalized ½ dram vials at 0 °C. In these experiments, crystals of α-polymorph grew on the walls of vials **1**-**8** after *10 days* and crystals of γ-polymorph appeared at the bottom of the **9** vials after two weeks. Again, these results clearly point to the ability of perfluoroalkyl surfaces to thwart the heterogeneous nucleation of metastable polymorph of indomethacin.

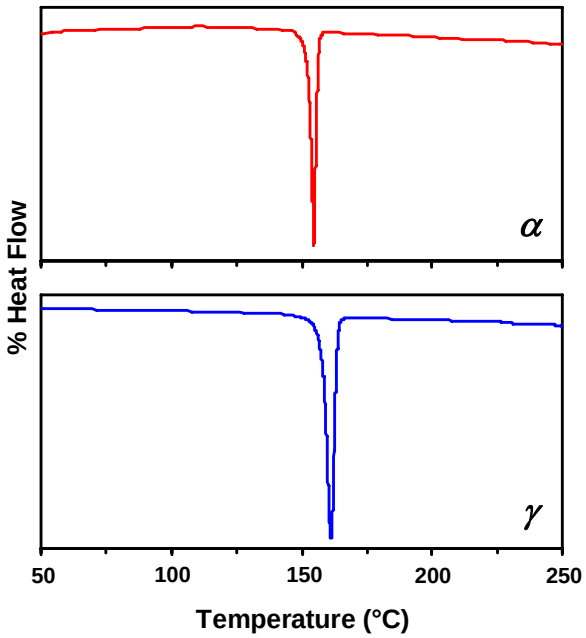

Figure S2. DSC Plots of α- (red, above) and γ-polymorphs (blue, below) showing the melting endotherms. Note that the γ-polymorph melts (158 °C) at a slightly higher temperature than the α-form (153 °C).

S10. Differential Scanning Calorimetry. These measurements were carried out with DSC-2920 (TA Instruments) in hermetically sealed and crimped aluminum pans. Samples were subjected to heating in the range 30-250 °C at a rate of 10 °C per minute (Figure S2). The two polymorphs showed distinct

endotherms corresponding to their melting; α at 153 °C and γ at 158 °C. These melting points are 2-3° less than the reported values in the literature. No other phase transitions were observed in the temperature range used.

S10. Infrared Spectra of Polymorphs. Infrared spectra were collected with a Nexus FT-IR spectrometer (Model 670) equipped with a liquid nitrogen cooled MCTA detector and an ATR accessory. We used IR as the first characterization tool because the ATR accessory allowed rapid data acquisition (< 1 min) with a small amount of sample (< 5 mg). The two polymorphs under consideration can be clearly identified from the IR spectra (Figure S3). The α-polymorph crystallizes in a noncentrosymmetric space group ($P2_1$) with three molecules in the asymmetric unit, whereas the γ-polymorph belongs to a centrosymmetric space group ($P\bar{1}$) with one molecule in the asymmetric unit. Consequently the α-polymorph has greater number IR absorptions than the γ-polymorph. A comparison of the two spectra reveals that there are several peaks that distinguish the two polymorphs; the arrows in Figure S3 indicate the characteristic absorptions used by other researchers to identify the α-polymorph.

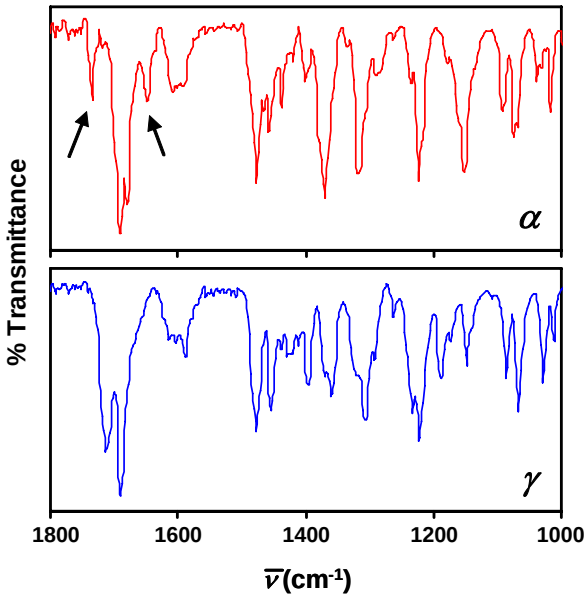

Figure S3. ATR-FT IR Spectra of α- (red, above) and γ-polymorphs (blue, below). Notice the significant differences between the two IR spectra; arrows in the top spectrum show characteristic peaks of α-polymorph.

S11. Powder X-Ray Diffraction Analysis. Powder X-ray data were collected on a Rigaku Geigerflex D-MAX/A diffractometer using Cu-$K\alpha$ radiation. The instrument was equipped with a vertical goniometer and a scintillation counter as a detector and applied Bragg-Brentano geometry for data collection. X-rays were generated at a power setting of 35 kV and 35 mA. Crystals of the α-polymorph were fluffy and small quantity of this polymorph occupied large volumes; the diffraction peaks of this polymorph were usually weaker than the γ-polymorph. The crystals obtained from the experiments above were pulverized using a mortar and a pestle prior to diffraction analysis. Finely ground powders were transferred to a glass sample holder that had loading dimensions 1.6 cm × 2 cm and exposed to X-rays over the 2θ range 5-40° in 0.05° steps and at a scan rate of 2° per minute. Figure S4 shows the experimental powder patterns along with powder patterns calculated from the single crystal X-ray structures. These X-ray patterns show that the crystals obtained from **9** vials correspond to the γ-polymorph.

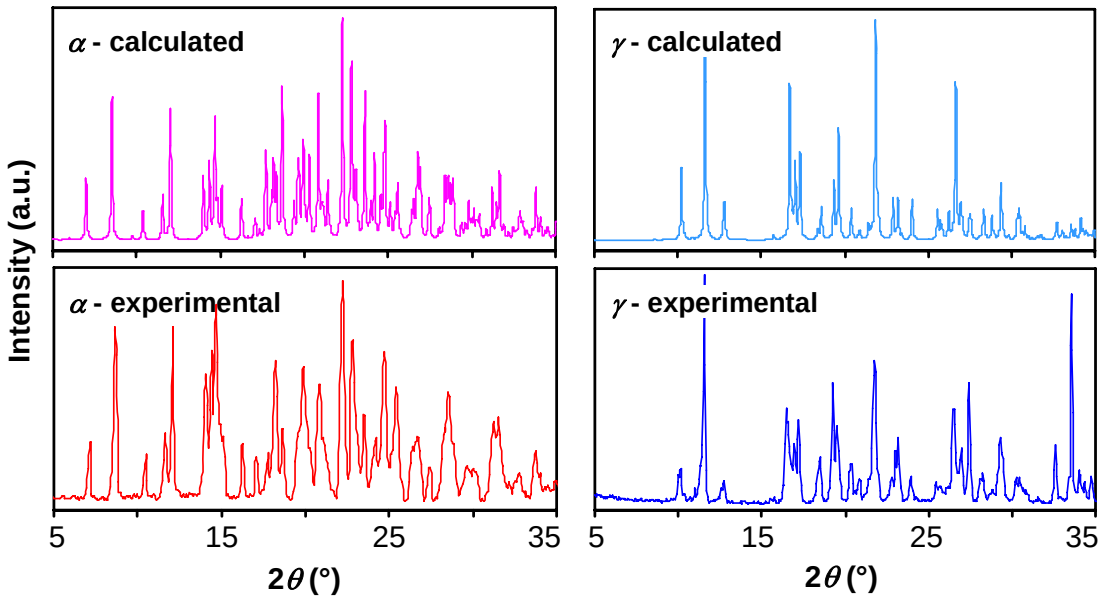

Figure S4. Calculated (top) and experimental (bottom) powder X-ray diffraction patterns of α- (left) and γ-polymorphs (right). The experimental diffraction pattern for the γ-polymorph is taken from the crystals grown in a **9** vial. The experimental diffraction pattern for the α-polymorph is taken from fibrous material collected from a **5** vial. These patterns match well with the diffraction patterns calculated from the single crystal structures.

S12. Quantitative Analysis of α- and γ-polymorphs. The crystals of α- and γ-polymorphs have distinct morphologies (see Figure S6); we could readily distinguish between the two forms by visual inspection. We separated the crystals of γ-polymorph grown on glass slides and vials (Sections S6 and S7) with the aid of a pair of tweezers, a surgical blade and microscope. We scraped the solid material from the vial on to a glass slide (50 × 75 mm), spread the crystals, and moved the γ-crystals to a different slide. These separated samples were then weighed on an analytical balance and the weights so obtained were used to calculate the relative amounts of the two polymorphs (Figure 4). Separation of this kind invariably left a small portion of α-form in the pile of γ-form and vice versa. This method is thus approximate and cannot be used for accurate quantitative analysis. The main result of the current study (exclusive growth of the crystals of γ-polymorph on **9** monolayers), however, is unaffected by the inaccuracies of this method. As noted in the main text, co-grinding of samples is a prerequisite for the quantification by PXRD and IR spectroscopy; such co-grinding can lead to phase transition between the polymorphs or transition to the amorphous form.

S13. Effect of Surface-to-Volume (S/V) Ratio of the Vial on the Crystal Growth. We performed all the experiments described in Section S7 (crystallizations in functionalized vials) using ½ dram vials. Owing to their small sizes, these vials have a high S/V ratio (5.61 cm^{-1}); crystallization in these vials is governed predominantly by heterogeneous nucleation on the surfaces (as opposed to the bulk nucleation in solution). The result in the case of **9** vials is that the nonstick perfluoroalkyl surfaces control the crystallization process: they prevent the attachment of nuclei of α-polymorph to vial walls and force the bulk nucleation of stable γ-polymorph (and further crystal growth of the stable polymorph at the expense of metastable α-polymorph by Ostwald ripening).

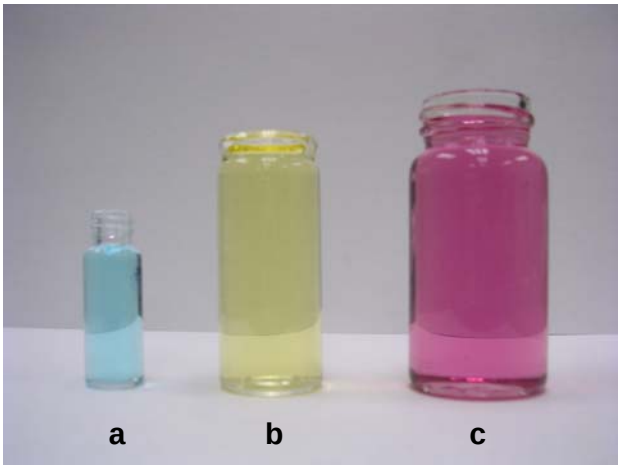

Figure S5. Glass vials (**a**: ½ dram; **b**: 3 dram; **c**: 20 mL) used for indomethacin crystal growth. The vials are filled with aqueous solutions of food dyes to accentuate the contrast between them. Most crystallizations in this work are performed in ½ dram vials.

We performed crystal growth experiments in larger vials with smaller S/V ratios (Figure S5). Seven of the eight crystallization experiments in 3 dram vials (S/V = 2.83 cm^{-1}) functionalized with **9** monolayers gave only the γ-polymorph. In one experiment, α-polymorph (6%) crystallized along with the γ-form. When 20 mL vials (S/V = 2.37 cm^{-1}) functionalized with **9** monolayers were used, crystals of α-polymorph appeared (4-13%) in six of the eight experiments. Two crystal growth experiments done in 100 mL beakers (S/V = 1.21 cm^{-1}) functionalized with **9** monolayers yielded α-polymorph (18% and 24%) along with the γ-polymorph in both the experiments. Thus, the current method is effective when vials with high S/V ratios are used for crystal growth. Our work shows that researchers aiming to crystallize stable polymorphs will have higher chances of success at their attempts if they use narrow tubular vessels (with high values of S/V ratios) functionalized with **9** or other related perfluoroalkyl monolayers. We believe that similar results can be obtained when vessels with nonstick coatings or vessels made of Teflon or other related materials are used for crystal growth. Fabrication of superhydrophobic surfaces is a thriving area of current research; we expect that application of these superhydrophobic surfaces for crystal growth will further improve capabilities of the method developed in this work.

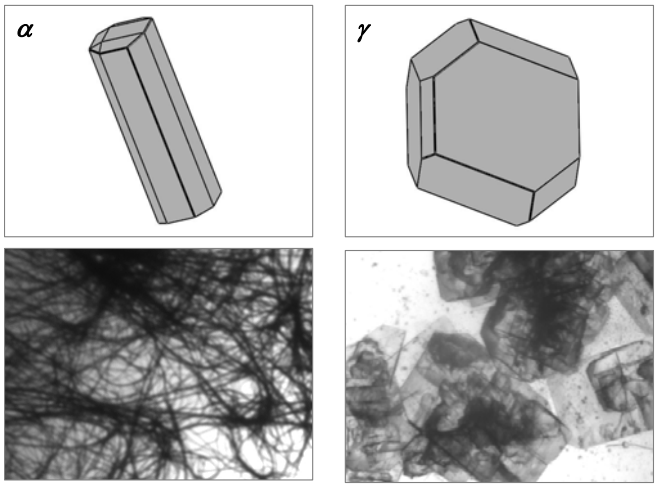

Figure S6. Calculated (top) and experimental (bottom) morphologies of α- (left) and γ-polymorphs (right) of indomethacin.

S14. Experimental and Calculated Morphologies of α- and γ-polymorphs. We noted in the main text and also in Section S12 that α- and γ-polymorphs have distinct morphologies. In our experiments, crystals of α-polymorph grew as very thin, fibrous needles and they usually appeared as clumps. In contrast, crystals of γ-polymorph grew as pseudohexagonal or nearly rectangular plates. Seldom, they also crystallized as rectangular needles or blocks. Crystals of γ-form also often grew as small clusters. This clustering of the crystals of both polymorphs and the stark differences in their morphologies allowed the easy separation of one polymorph from another by hand. Figure S6 shows experimental morphologies of both the polymorphs along with the morphologies calculated using BFDH (Bravais-Friedel-Donnay-Harker) theory.

S15. Enlarged Microscopic Images. Here we show the enlarged versions (Figures S7 and S8) of the microscopic images shown in the main text. At the scale shown here it is possible to see the crystals of two polymorphs clearly. We use these enlarged images to show the locations of growth of the two polymorphs.

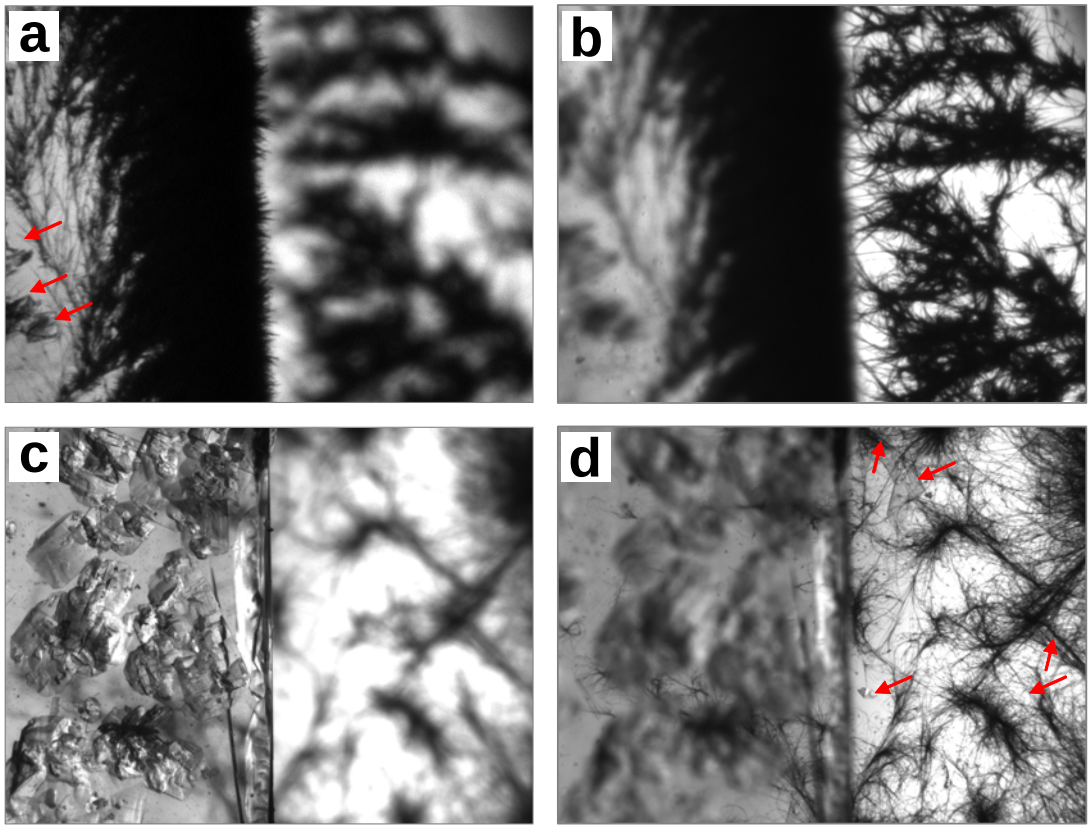

Figure S7. Enlarged version of Figure 3 in the main text. Indomethacin crystal growth using method-1. Slides coated with silane monolayers are on the left side of the images. The right portions of the images show bottoms of the vials not covered by the slides. (**a**-**b**) Crystal growth on **5** monolayers with focus on the slide (in **a**) and on the vial (in **b**). Notice the predominant growth of α-polymorph on both locations. (**c**-**d**) Crystal growth on **9** monolayers with focus on the slide (in **c**) and on the vial (in **d**). Notice the predominant growth of γ-polymorph on the slide and α-polymorph at the bottom of the vial. Arrows show some of the crystals of γ-polymorph crystallized along with the α-polymorph.

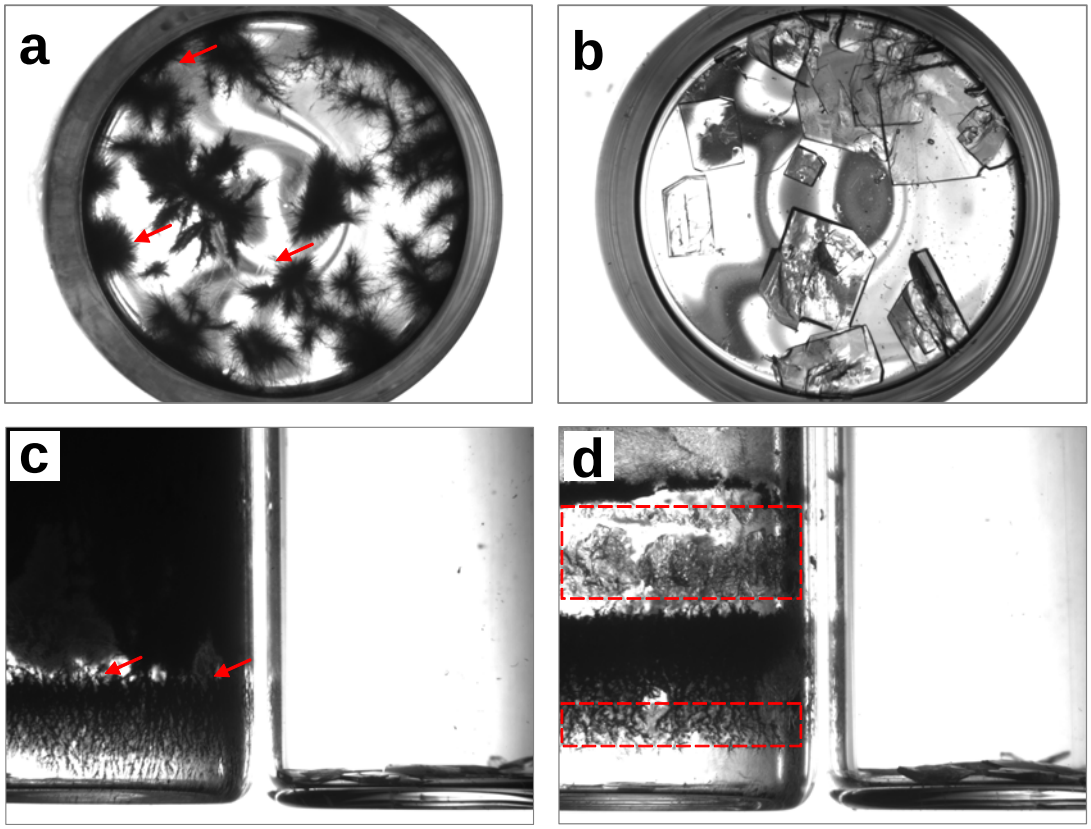

Figure S8. Enlarged version of Figure 5 in the main text. Indomethacin crystal growth using method-2. (**a**-**b**) View perpendicular to the bottom of the vial showing the crystal growth on **5** (in **a**) and **9** (in **b**) monolayers. In this zoomed out view only α-crystals are seen in **a**. At a closer view, this vial contains ~10 % of γ-crystals. Notice the exclusive growth (and larger size) of γ-crystals in **b**. (**c**-**d**) View parallel to the bottom of the vial showing the crystals grown on **5** (left vial) and **9** (right vial) monolayers in ethanol (**c**) and acetonitrile (**d**) solutions. Notice the rampant crystal growth of α-form on the walls of **5** vials. In contrast, crystal growth is completely inhibited on the walls of **9** vials. Notice the plate-like γ-crystals at the bottoms of **9** vials. Arrows and boxed areas show some of the crystals of γ-polymorph crystallized along with the α-polymorph.